Mesoscopic Computational Haemodynamics

Artoli, A.M.M.

Publication date
2003

Chapter 5

Pulsatile Flow Benchmarks

In the last chapter, we have shown that the lattice BGK works well for steady flow benchmarks. The advantages and drawbacks of the method were discussed in Chapter 2. In this chapter, detailed analysis of the accuracy of the lattice BGK method in simulating pulsatile flow in a 2D channel and a 3D tube is presented. The influence of different boundary conditions on the accuracy is discussed.

5.1 Introduction

Recently, it has been demonstrated that the lattice BGK method is useful to simulate time-dependent fluid flows (Krafczyk *et al.*, 1998). As demonstrated in Chapter 2, for steady flow, the lattice BGK is second order accurate in the velocity fields and the stress tensor, when second order boundary conditions are applied. Although the accuracy has been studied extensively for steady flows, studies on the accuracy of lattice BGK for time dependent flows are quite rare (He and Luo, 1997; Artoli *et al.*, 2002c).

Pulsatile flow characteristics are quite important in haemodynamics. It is believed that the shear stress and other haemodynamic factors play a dominant role in diagnosis and treatment of cardiovascular diseases (e.g. Wooton and Ku, 1999). These factors are either studied by building experimental or simulation models for locations of interest. Depending on the geometry of these locations, appropriate approximations such as rigidity of the wall, circular cross section and assuming blood to behave as a Newtonian fluid commonly take place. The role of Computational Haemodynamics is well recognised in this field and proved to be of great help in understanding the nature of blood flow in diseased locations (Vorp *et al.*, 2001).

As mentioned before, with lattice BGK, it is possible to compute the local components of the stress tensor without a need to estimate the velocity gradients from the velocity profiles. In addition, the equation of state defines the pressure as a linear function of the density, which makes it easy to obtain the pressure from the density gradient. All these advantages make the lattice BGK a suitable candidate for simulating time-dependent blood flow in arteries.

In this chapter, we investigate the accuracy of the lattice BGK model in recovering analytical solutions for oscillatory two dimensional (2D) channel flow and three dimensional (3D) tube flow. The 2D simulations are performed to test and validate the model, while the 3D simulations are performed to model a straight rigid segment of a large artery. Typical values from haemodynamics are used to cover a range of Womersley and Reynolds numbers.
The standard lattice BGK model works well as long as the Mach number M is low ($M^2 << 1$) and the density fluctuations are small. However, modelling unsteady flows involves higher density fluctuations, since the only way to model time-dependent pressure in lattice BGK is by incorporating time-dependent density. Also, compressibility errors at high Mach numbers are expected. It has been reported that, with compressible lattice BGK models, when the pressure gradient is time-dependent, compressibility effects may arise and using an incompressible model is necessary (He and Luo, 1997). Realizing this defect, other incompressible lattice BGK models have been developed (Zou *et al.*, 1995; He and Luo, 1997; Guo *et al.*, 2000) here referred to as D2Q9i, D2Q9ii and D2Q9iii, respectively. The difference between the D2Q9 and the D2Q9i is that the density in the equilibrium distribution is inside the brace of Eq. (3.4) for the D2Q9i. The D2Q9ii assumes the pressure to be the independent dynamic variable instead of the density, and is equivalent to D2Q9i when the density is equal to unity. The D2Q9iii introduced a different equilibrium distribution function with which it is possible to exactly derive the incompressible Navier-Stokes equations in the limit of a low Mach number. As the incompressible D2Q9i model has already been tested for steady flows, for which it was proposed, we test it here for unsteady flows after noting that the D2Q9i is a special case of the D2Q9ii.

5.2 Boundary Conditions

As stated before, with the lattice Boltzmann methods, the no-slip boundary condition is not automatically recovered at the boundaries. Therefore, the walls require special treatment. A number of boundary conditions have been proposed which are either of first or second order accuracy in space and may or may not have slip velocities at the walls. In this study, we distinguish four types of wall boundary conditions:

1. The bounce-back on the links, referred to later as BBL, in which particles coming to the walls simply return back to the fluid in the direction where they came from. Collision is not performed at the boundary nodes while using this boundary condition. It is simple, computationally efficient, and can be used for a complex geometry, but is of first order and is known to yield a slip velocity which in turn can be minimised by increasing the grid size and tuning the viscosity.

2. The bounce-back on the nodes, referred to as the BBN, in which collision is allowed at the boundary nodes. The bounce-back on the nodes is known to be of second order accuracy, but still has a slip velocity, except when $\tau = 1$.

3. Recently, Bouzidi *et al.* (2001) introduced another version of the bounce-back on the links which allows using the bounce back for the curved geometry, and we will refer to it as the bounce back on a curved boundary (BBC). The idea of this boundary condition is to add a linear or a quadratic interpolation term to the streaming step by considering the first or both the first and the second fluid points together with the bounce back rule. The bounce-back on the links is a special case of this boundary condition.

4. The non-slip velocity and pressure boundary conditions presented by Zou and He (1997) have been used to set a specific velocity or pressure at the boundary by assuming that the bounce-back is valid for the non-equilibrium parts of the distribution functions and explicitly computing the unknown distributions.

5.3 Simulations in 2D

We have conducted a number of 2D simulations for time dependent flow in a channel. Various boundary conditions have been tested. For the walls, we have used the bounce-back on the nodes and non-slip boundary conditions; for the inlet and outlet, we have used periodic boundaries in combination with body forcing or velocity and pressure boundaries. For all simulations described below, unless otherwise specified, the flow is assumed to be laminar ($R_e < 2000$) and the Mach number is assumed to be low ($M < 0.1$).

5.3.1 Oscillatory Channel Flow

We have studied the flow in an infinite 2D channel due to an oscillatory pressure gradient $\frac{\partial P}{\partial x} = Asin(\omega t)$, where A is a constant. The pressure gradient is implemented by applying an equivalent body force G or by appropriate oscillating pressure difference between the inlet and outlet. The analytical solution for the velocity in this case is given by the Real part of (Pozrikidis, 1997)

$$v(y,t) = -\frac{A}{\rho\omega} e^{-i\omega t} \left(1 - \frac{cosh\left[\sqrt{b}(y - L/2)\right]}{cosh\left[\sqrt{b}L/2\right]} \right) \tag{5.1}$$

where ρ is the fluid density, L is the width of the channel, and $b = -i\omega/\nu$.
To check the accuracy of the lattice BGK model, we have performed a number of simulations. The Reynolds number is defined as $R_e = \frac{UL}{\nu}$, the Womersley number is defined as before; $\alpha = R\sqrt{\frac{\omega}{\nu}}$, and the Strouhal number is defined as $St = \frac{R}{UT}$, where $R = L/2$, ν is the kinematic viscosity, $\omega = \frac{2\pi}{T}$ is the angular frequency and T is the sampling period. The velocity U is given by $U = -\frac{-1}{2\nu\rho}\frac{dp}{dx} \equiv \frac{L^2 G}{8\nu\rho}$, the average density of the system is $\rho = 1.0$ and the pressure gradient is sinusoidal with amplitude A.

At first, we have used the bounce-back on the nodes (BBN) which is quite simple and is known to be of second order accuracy. Periodic boundary conditions are used for the inlet and the outlet boundaries. Both the Reynolds and the Womersley numbers were kept fixed by fixing the distance L between the two plates and varying the relaxation parameter τ, the period T and the body force G. The error in velocity at each time step is defined by

$$Ev = \frac{\sum_{i=1}^{n} |\vec{v}_{th}(\vec{x}_i) - \vec{v}_{lb}(\vec{x}_i)|}{\sum_{i=1}^{n} |\vec{v}_{th}(\vec{x}_i)|} \tag{5.2}$$

where $\vec{v}_{th}(\vec{x}_i)$ is the analytical solution for the horizontal velocity, $\vec{v}_{lb}(\vec{x}_i)$ is the velocity obtained from the lattice BGK simulations and n is the number of lattice nodes representing the width of the channel. The overall average error, $< Ev >$, is averaged over the period T. The relaxation time ranges from $\tau = 0.6$ to $\tau = 3.0$, the body force ranges from $G = 25 \times 10^{-5}$ to $G = 0.04$ and the sampling period lies in the range $500 - 20$, giving corresponding values of $0.2 - 5.0$ for δ_t, with $\delta_t = 1$ corresponding to the case where $\tau = 1$. The system was initialised by setting the velocity to zero everywhere in the system. The convergence criterion is attained by comparing simulation results from two successive periods and the stop criterion is when this difference is less than 10^{-7}. The agreement between the simulation and the analytical solutions is quite good, as is shown in Fig. 5.1 in which the obtained velocity profiles (point) for $\alpha = 4.34$ at $t = 0.75T$ are compared to the theory (dashed line). However, there seems to be a small shift in time between the simulation and the theory. This shift is a function of time and τ. We have found that if we assume that the theory lags the simulation with a half time step, i.e $t_{lb}\delta_t = t_{th} + 0.5\delta_t$, the error reduces at least one order of magnitude for all τ values. Figure 5.1 shows a typical simulation result compared to the analytical solution with (solid line) and without (dashed line) shifting the time coordinate. We have used this observation to compare the simulation results with the shifted analytical solution which leads to excellent agreement for all values of time, as shown in Fig. 5.2 The error as a function of time is shown in Fig. 5.3 from which it can be seen that the error is minimum at $\tau = 1$, since there is no slip velocity at this specific case (He *et al.*, 1996). An error of the order of the round-off error could be reached for the special case when $\tau = 1$, when the bounce-back on the nodes is used, and assuming the 0.5 time shift (the asterisks, *, in Fig. 5.3). From Fig. 5.3 we also observe that the error is maximum at a quarter period in time. This may be attributed to the large pressure gradients at this time.

This shift in time has been observed before by Matthaeus (2001). It may be attributed to the way the driving force is imposed in the simulation and details of the specific lattice BGK model (force evaluation). We also believe that the way in which time coordinates are discretised may have some effects on this shift. For the other cases, when $\tau \neq 1$, the effect of the slip velocity dominates. Up to now, the slip velocity has analytical expression for the steady channel flow, but not yet for the unsteady flow. In the next sections we will investigate the influence of boundary conditions and flow parameters such as the Reynolds number on this shift.

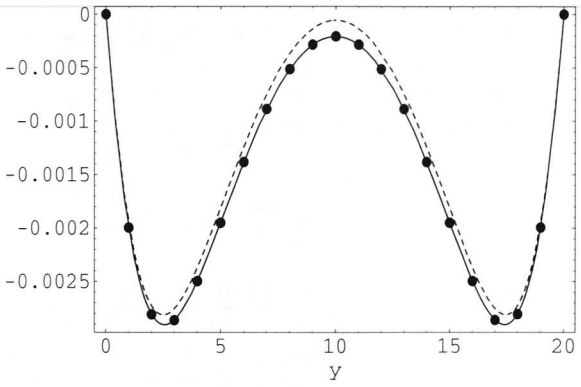

Figure 5.1: Velocity profile (in Lattice Units) at $t = 0.75T$ with $\tau = 1$, $\alpha = 4.34$, $R_e = 10$ and $St = 0.6$ in a 2D oscillatory channel flow using the BBN. The dots are the lattice BGK results. The dashed line is the analytical solution and the solid line is the analytical solution with a shift of 0.5 time step.

5.3.2 Non-Slip Boundary Conditions

In order to remove errors arising from the slip velocity, we have conducted similar simulations with the no-slip velocity boundary conditions explained in section 5.2(4) at the walls and periodic boundary conditions at the inflow and the outflow boundaries. The body force that corresponds to a desired Reynolds number drives the flow. The Strouhal number is kept constant by fixing both the Reynolds and the Womersley numbers and looking at the accuracy in time. This is done by fixing the width L and assigning the corresponding values for the sampling period T, the body force G, and the relaxation parameter τ. In this way, δ_t will change. The results are shown in Fig. 5.4 which shows the average error $< Ev >$ as a function of δ_t. From this figure, we clearly see that the lattice BGK is of first order accuracy in time (slope = 0.9). The error is again decreased when the half-time step correction is used, specially at $\tau = 1$, as shown in the same graph. From this experiment, we conclude that the shift in time does not depend on the used boundary condition.

5.3.3 Influence of the Reynolds Number

We have conducted another set of simulations to see the influence of the Reynolds number on the error in the flow fields. Here, the relaxation parameter is kept fixed at the value $\tau = 1$, the width of the channel is varied to achieve higher Reynolds numbers and the period is changed accordingly to keep the Womersley parameter constant. The length of the channel is $5L$. In summary, we change the Reynolds

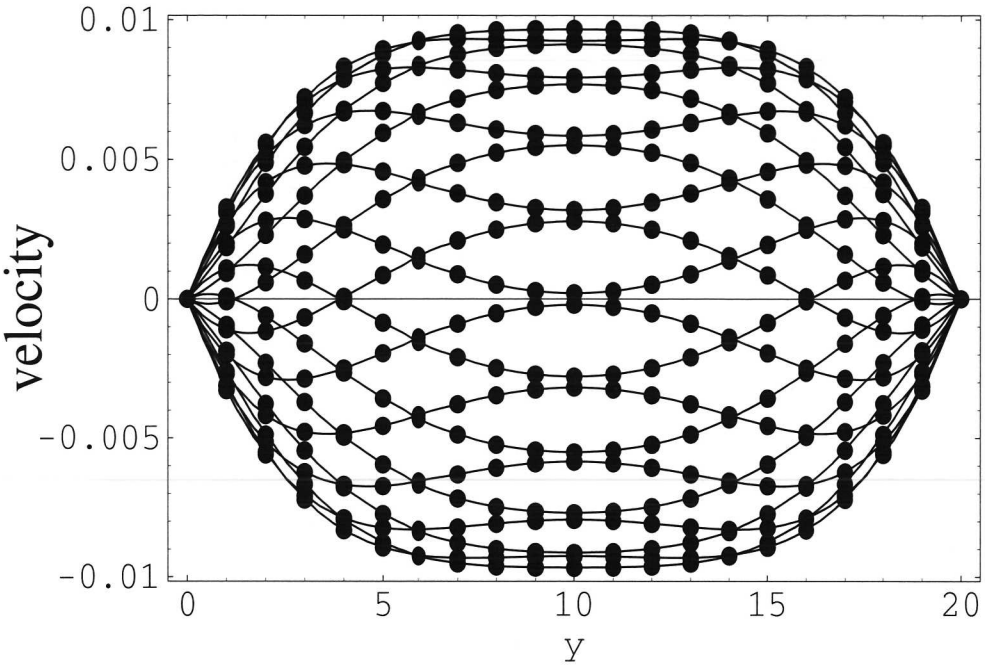

Figure 5.2: Obtained velocity profiles (in Lattice Units) over a complete period (dots) compared to the shifted theory (lines) with $\tau = 1$, $\alpha = 4.34$, $R_e = 10$ and $St = 0.6$. The measurements are taken at the middle of the channel, at each $t = 0.05nT$ where $n = 0, 1, ..., 20$.

number R_e, the body force G, the width L and the period T. Simulations for Reynolds numbers in the range $1 \rightarrow 200$ at $\alpha = 15.533$ were performed. Figure 5.5 shows comparisons of numerical and analytical solutions of the velocity profile for $R_e = 200$ at $t = 0.2T$. Similar agreements between theory and simulations have been observed for the whole period at different Reynolds numbers (data not shown). When compared to the analytical solutions, with and without shift in time, the error decreases from $< Ev >= 0.0085$ to $< Ev >= 0.00024$ for $R_e = 200$.

We observe that the difference between the two analytical solutions (the original and the shifted) becomes less as the Reynolds number increases. This suggests that the shift is inversely proportional to the applied body force which may have direct influence on it. It is therefore necessary to conduct another set of simulations in which the body force has no influence (i.e. is absent).

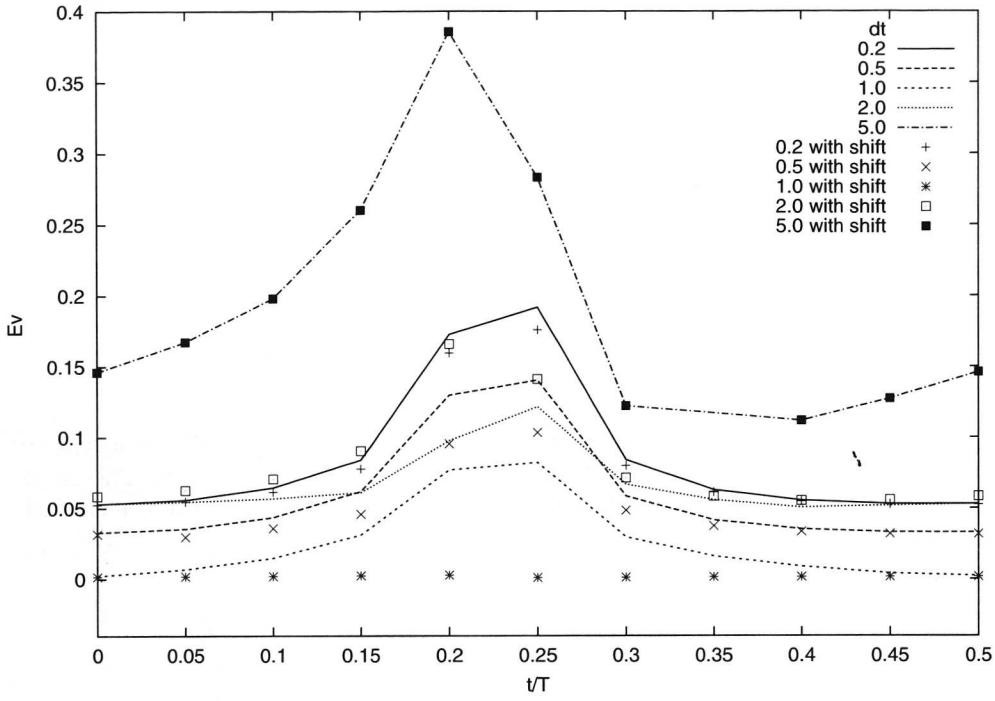

Figure 5.3: Error behaviour over a half cycle for different values of δ_t as a function of the fractional time t/T without (lines) and with (points) time-shift correction for $\alpha = 4.34$, $R_e = 10$ and $St = 0.6$ in a 2D oscillatory tube flow using the BBN boundary condition.

5.3.4 Inlet and Outlet Pressure Boundary Conditions

In order to remove the influence of the body force, we have conducted another set of simulations in which the flow in a 2D channel is driven with a sinusoidal pressure gradient of magnitude $A = 0.001/L_x$ where L_x is the length of the channel. The length of the channel is 10 times the width and the period of the driving pressure is $T = 1000$. The density at the inlet is $1 + Asin(\omega t)$ and is set to be 1.0 at the outlet. The convergence criterion is attained by comparing simulation results from two successive periods with a stop criterion less than 10^{-7}. All the flow fields were initialised from zero. We have again observed good agreement with the theory, as is shown in Fig. 5.6 The shift in time has diminished in magnitude, but it is still there ($< Ev >= 0.019$ without shift and reduces to $< Ev >= 0.017$ with shift).

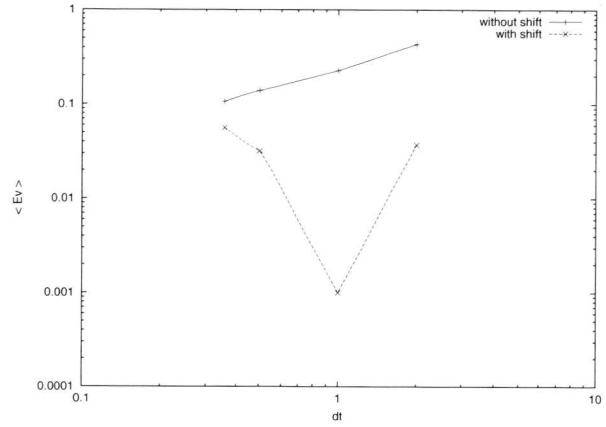

Figure 5.4: Relative Error in velocity, averaged over the whole period, versus the time step for $\alpha = 15.53$, $R_e = 10$ and $St = 7.68$ in a 2D oscillatory channel flow. The slope of the straight line is 0.90. The dashed line is the error with reference to the shifted in time analytical solution. A second order BBN boundary condition is used here.

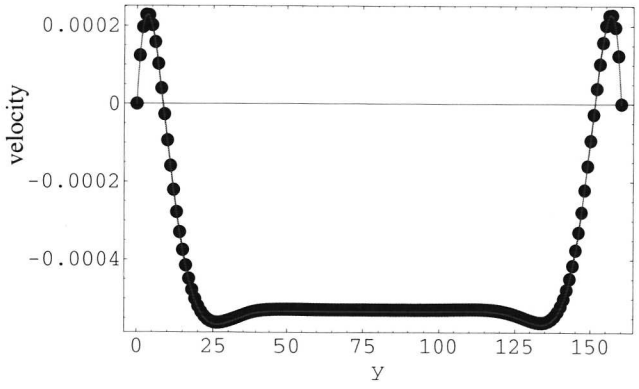

Figure 5.5: Velocity profiles (in Lattice Units) obtained from lattice BGK simulations (dots) for $\alpha = 15.53$, $R_e = 200$ and $St = 0.38$ in a 2D oscillatory channel flow, showing excellent agreement with the analytical solutions (lines). The effect of time shift is not observable.

5.4 Simulations in 3D

To have a complete picture about the accuracy of the lattice BGK, we have conducted a number of 3D simulations of sinusoidal flow in a tube using a parallel lattice BGK

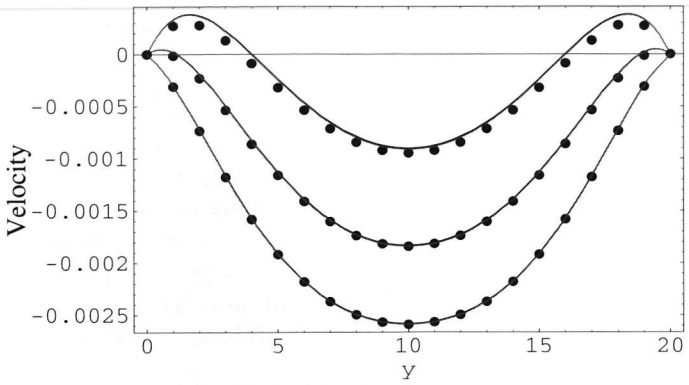

Figure 5.6: Velocity profiles obtained from lattice BGK simulations (dots) for $\alpha = 4.00017$, $R_e = 10$ and $St = 0.51$ in a 2D oscillatory channel flow when inflow and outflow boundary conditions are used. Selected simulation times are shown. The shift in time has little effect but is still there.

solver developed in our group (Kandhai *et al.*, 1998) with added functionalities for dedicated in- and outlets, solid boundary and shear stress calculations (Artoli *et al.*, 2002). The diameter of the tube is represented by 39 lattice nodes and the minimum tube length is $L = 50$ lattice nodes. First, we have used the BBL together with periodic boundaries to simulate oscillatory flow in the tube. The simulation period is set to be $T = 800$, the relaxation parameter is $\tau = 0.625$ and the amplitude of the body force G is chosen to be 4.687×10^{-6} in order to have a Womersley number $\alpha = 8.4661$. Initialisation of the system and the stop criterion is the same as that for the 2D case. The simulations were performed on 4 nodes of a Beowulf cluster using slice decomposition. The time per iteration is about 0.2 seconds.
The obtained velocity profiles for a half cycle are shown in Fig. 5.7, compared to the analytical solution

$$u(y,t) = Re\left[-\frac{A}{\rho\omega}e^{-i\omega t}\left(1 - \frac{J_0\left[\sqrt{b}y\right]}{J_0\left[\sqrt{b}R\right]}\right)\right], \tag{5.3}$$

where J_0 is the zeroth order Bessel function of the first type and again $b = -i\omega/\nu = -i(\alpha/R)^2$. Similar velocity profiles have been obtained for the complete period and for a range of Womersley parameters and relaxation times. The overall average error is about 15 % and is maximum at the centres and near to the walls where the flow reverses. This large error may be attributed to, among others, the stairing geometry of the boundary, the way of implementation of the body force, the slip velocity of the bounce back rule and the compressibility effect.

There are at least two ways to reduce the error; to use an incompressible 3D model, and/or to have more advanced boundary conditions. As there exist more advanced boundary conditions which are well tested (see for e.g. (Zou and He, 1997; Mei *et al.*, 1999; Bouzidi *et al.*, 2001), as a first step, we have applied the curved boundary conditions recently proposed by Buzaidi *et al.* (2001) which is simple and easy to implement. It has been realised by the author that the Bouzidi boundary condition slightly violates mass conservation. This has a very little effect on the final solution. With the curved boundaries, the system size and the simulation parameters are the same as those for the bounce-back. The accuracy is significantly enhanced, as shown in Fig. 5.4 which shows both the simulation results (points) and the analytical solutions. The shift in time was not clearly observed here. This may be attributed to the different nature of the quasi compressible D3Q19 Model in which we have combined errors from stairing and compressibility effects.
The error behaviour is studied by keeping fixed both the Reynolds and the Womersley numbers via fixing the diameter R and varying the relaxation time τ, the body force G and the period T. Defined as above, the error behaviour as a function of the sampling period is shown in Fig. 5.9, from which we observe that the error enhances as the number of sampling points representing the period increases. This is expected as the time step decreases with increasing T. The error behaves as first order in time (slope of the fitted line is about 1.0). Furthermore, as a typical Reynolds number in the Abdominal aorta is 1250 we have performed another set of simulations at this Reynolds number with $\alpha = 7.7284$ by setting $T = 1200$ and $\tau = 0.6$. Figure 5.10 shows the simulation results compared to analytical solutions. The average error per time step is about 0.07 which is in the worse case still two times more accurate than when the BBL is used, even if they are both of first order accuracy. As we are interested in blood flow simulations, periodic boundary conditions are not suitable, since there are different flow conditions at the outlets of the arteries. Therefore, we have tried an inlet-outlet boundary condition in which we have assumed stagnant flow at the inlet and no flux at the outlet. This is done by copying the densities from inside the flows to the inlet and the outlet, computing the velocity near the outlet and assigning equilibrium distributions to the outlet distribution functions, and applying a body force or a pressure gradient to drive the flow. We have obtained comparable results for periodic boundary conditions (the difference in error is about 0.004).

5.5 Shear Stress

As mentioned previously, the shear stress is an important factor in haemodynamics and is known to play a dominant role in the localisation of cardiovascular diseases such as atherosclerosis. We have shown in a previous article (Artoli *et al.*, 2001) that the components of the stress tensor in the lattice Boltzmann BGK method can be computed from Eq. (3.22)

$$\sigma_{\alpha\beta} = -\rho c_s^2 \delta_{\alpha\beta} - \left(1 - \frac{1}{2\tau}\right) \sum_{i=0} f_i^{(1)} e_{i\alpha} e_{i\beta}. \tag{5.4}$$

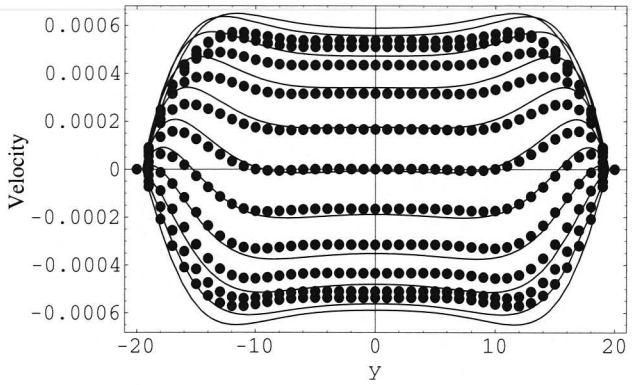

Figure 5.7: Obtained velocity profiles (dots) compared to the analytical Womersley solutions (lines), for $\alpha = 8.4661$ and $R_e = 10$ in a 3D oscillatory tube flow using the bounce-back on the links. The overall average error is about 15%.

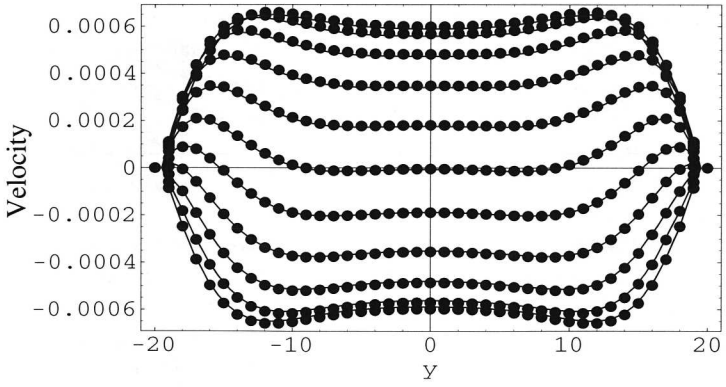

Figure 5.8: Obtained velocity profiles (dots) compared to the analytical Womersley solutions (lines), for $\alpha = 8.4661$, $R_e = 10$ and $St = 2.2815$ in a 3D oscillatory tube flow using the BBC. The overall average error is about 7 %.

in lattice units, where the quantity $f_i^{(1)} e_{i\alpha} e_{i\beta}$ is usually computed during the collision process. Therefore, the stress tensor components can be obtained without almost any additional computational cost. This extensively enhances the lattice Boltzmann BGK method, as other CFD methods are more elaborate and estimate the stress tensor components from the simulated velocity field. We have used this formula to compute the shear stress for pulsatile flow and compare the simulation results with the ana-

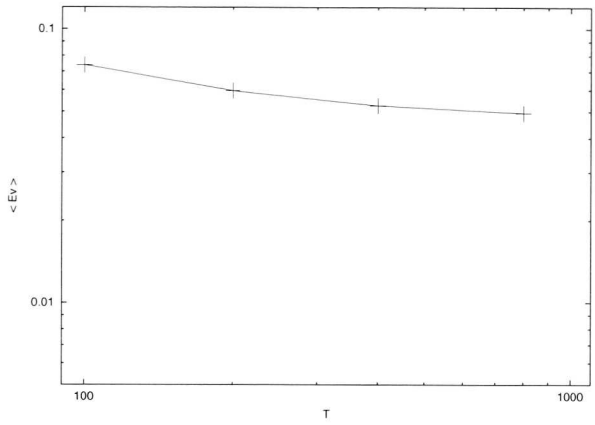

Figure 5.9: First order error behaviour as a function of T at $\alpha = 8.4661$, $R_e = 10$ and 2.2815 for a 3D oscillatory tube flow with the curved bounce back and linear interpolation.

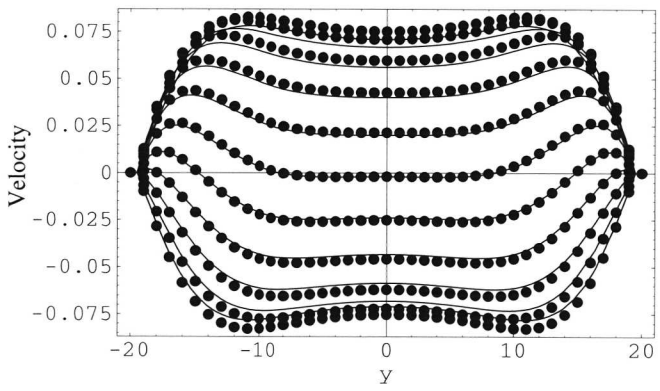

Figure 5.10: Velocity profiles with $\tau = 0.6, T = 1200, d = 39$, $\alpha = 7.7284$, $R_e = 1250$ and $St = 0.0152$ in a 3D oscillatory tube flow. The dots are the lattice BGK results with BBC boundary condition. The lines are the analytical solutions

lytical solutions derived from analytical velocity profiles. With both BBL and BBC, excellent agreements have been obtained for both the oscillatory channel (see Fig. 5.11) and tube flows (see Fig. 5.12). The shear stress vanishes in the canter and grows up towards the walls, where the velocity gradients are large. As the Womersley parameter increases, the flat region increases and the shear stress decreases in

the central region. Similar agreement with the theory has been obtained for the other stress components in a range of Womersley and Reynolds numbers. The shift in time has no effect here and is absent during the collision process. We have noticed that the shear stress is slightly better when the bounce-back on the links is used. The average error is about 0.18 for the BBL and 0.19 for the BBC. This may be attributed to the fact that the spatial gradient of the slip velocity vanishes which enhances the BBL over the BBC which interpolates in a region of high velocity gradients.

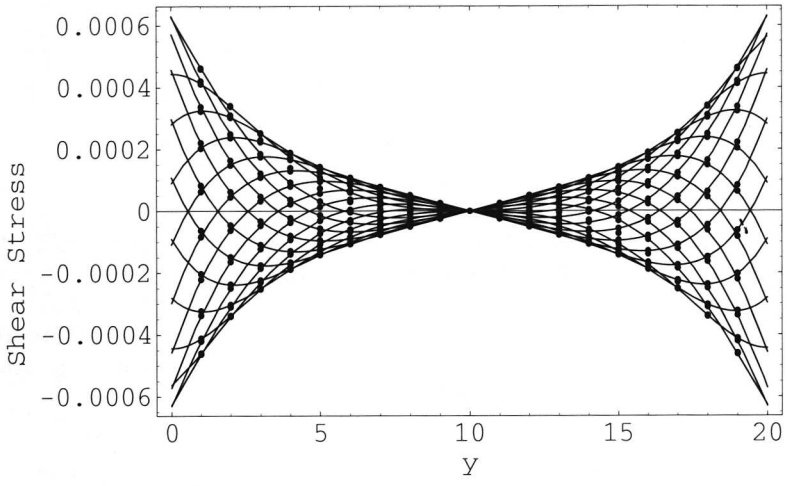

Figure 5.11: Shear stress (in Lattice Units) obtained from lattice BGK simulations (dots) for $\alpha = 4.34$, $R_e = 10$ and $St = 0.6$ in a 2D oscillatory channel flow, showing excellent agreement with the analytical solutions (lines). The effect of time shift is not observable.

5.6 Discussion and Conclusions

In this study, it has been shown that the lattice Boltzmann BGK model can be used to simulate time dependent flows in 2D within acceptable accuracy if suitable simulation parameters and accurate boundary conditions are used. We have conducted a number of 2D simulations for time-dependent flow in a channel with different boundary conditions. A shift in time has been observed and analysed. The lattice Boltzmann BGK model is more accurate when a half time step correction is added to the time coordinates. We have investigated the time shift association with the used boundary conditions, and have found that it is always present for the cases we have studied. However, the origin of this shift is not fully understood and is a subject for future research. The effects of the Womersley, the Reynolds and the Strouhal numbers have

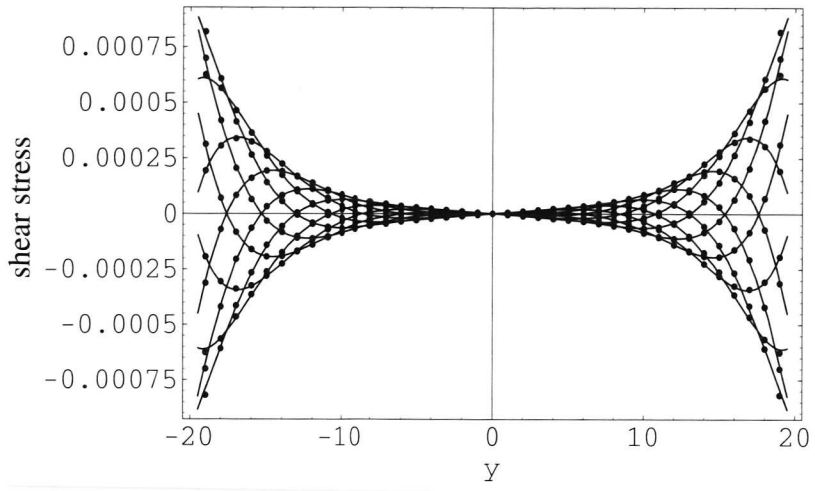

Figure 5.12: Shear stress (in Lattice Units) obtained from lattice BGK simulations (dots) for $\alpha = 7.7284$, $R_e = 1250$ and $St = 0.0152$ in a 3D oscillatory tube flow, showing excellent agreement with the analytical solutions (lines). The measurements are taken at each t = 0.1 nT where n = 0,1, ...,20.

also been studied in a number of simulations which showed that the shift in time is reduced at high Reynolds numbers. The obtained accuracy in time for time-dependent flows is of first order.

A quasi-incompressible D3Q19 model for the 3D simulations of oscillatory tube flow has recovered the analytical Womersley solution with average error of 15% when the bounce-back on the links boundary condition is used. The large error associated with the simple bounce-back rule may be attributed to the slip velocity, stair casing geometry and compressibility of the used lattice BGK model. The D3Q19 has been cited in the literature to result in large errors (He and Luo, 1997) when it is used to simulate time dependent flows, since the effect of the order $O(M^2)$ has to be taken into consideration. Incompressible models are encouraged and are under development in our group.

The bounce-back on a curved boundary recently proposed by Bouzidi *et al.* with linear interpolation has reduced the error to less than seven percent and didn't enhance the accuracy in the stress tensor calculations due to high velocity gradients close to the walls.

However, it has been reported that the lattice Boltzmann BGK model is thermodynamically inconsistent and that the forcing term leads to an incorrect energy balance equation if the acceleration is not constant in space (Luo, 2000). Therefore, it is argued that, it is better to use a general lattice Boltzmann model rather than the lattice BGK to overcome problems arising from artifacts in the lattice BGK model, since it

is not suitable for dense gases. Using the modified Lattice Boltzmann method that is derived from the Enskog equation confirms a proof of the Boltzmann H theorem and the forcing term recovers correct energy balance equations (Luo, 2000). On the other hand, the lattice BGK is simple and could yield satisfactory results if being used cautiously.